Journal of Hazardous Materials 161 (2009) 753–759

Contents lists available at ScienceDirect

Journal of Hazardous Materials

journal homepage: www.elsevier.com/locate/jhazmat

Spent tea leaves: A new non-conventional and low-cost adsorbent for removal of basic dye from aqueous solutions

B.H. Hameed*

School of Chemical Engineering, Engineering Campus, Universiti Sains Malaysia, 14300 Nibong Tebal, Penang, Malaysia

ARTICLE INFO

Article history:
Received 24 January 2008
Received in revised form 6 April 2008
Accepted 7 April 2008
Available online 11 April 2008

Keywords:
Spent tea leaves
Adsorption
Isotherm
Methylene blue
Kinetics

ABSTRACT

In the present study, spent tea leaves (STL) were used as a new non-conventional and low-cost adsorbent for the cationic dye (methylene blue) adsorption in a batch process at 30 °C. Equilibrium sorption isotherms and kinetics were investigated. The experimental data were analyzed by the Langmuir, Freundlich and Temkin models of adsorption. The adsorption isotherm data were fitted well to the Langmuir isotherm and the monolayer adsorption capacity was found to be 300.052 mg/g at 30 °C. The kinetic data obtained at different initial concentrations were analyzed using pseudo-first-order, pseudo-second-order and intraparticle diffusion equations. The results revealed that the spent tea leaves, being waste, have the potential to be used as a low-cost adsorbent for the removal of methylene blue from aqueous solutions.

1. Introduction

Textile dyeing is a major industry in Malaysia and consumes large quantity of water and produces large volumes of wastewater from different steps in the dyeing and finishing processes. Synthetic dyes are usually released into the environment from such industrial effluents and the discharge of highly colored synthetic dye effluents can be very damaging to the receiving water bodies. Moreover, dyes used in the textile industry may be toxic to aquatic organisms and can be resistant to natural biological degradation. Hence, the removal of color synthetic organic dyestuff from waste effluents becomes environmentally important. Consequently, many treatment processes have been applied for the removal of dyes from wastewater. These processes include: solar photo-Fenton degradation [1], photocatalytic degradation [2], photo-Fenton processes [3], biodegradation [4], integrated chemical–biological degradation [5], electrochemical degradation [6] and adsorption [7].

Adsorption process using suitable adsorbent has shown high efficiency for removal of dyes. Adsorption on activated carbon is the most widespread technology used in removal of dyes [8,9], phenols [10,11] pesticides [12], and other hazardous chemicals [13,14] which may be found in wastewater, but its high cost limits its commercial application. In recent years, extensive research has been undertaken to develop alternative and economic adsorbents. Such alternatives include palm ash [15,16], chitosan/oil palm ash composite beads [17], pomelo (*Citrus grandis*) peel [18], pumpkin seed hull [19], broad bean peels [20], oil palm trunk fibre [21], durian (*Durio zibethinus Murray*) peel [22], sodium montmorillonite clay [23], salts-treated beech sawdust [24], chitosan bead [25], biomass fly ash [26], zeolite [27] and almond shells [28].

Tea is basically the dried and processed leaves of only one species of plant called *Camellia sinensis* [29]. It is consumed by the largest number of people in the world and considered the second most popular beverage in the world. Only water is rated higher in world consumption than tea. It is estimated that somewhere between 18 and 20 billion cups of tea are drunk daily on our planet. Canned or bottled tea drinks as well as instant tea drinks are produced on industrial scale by hot water extraction of tea leaves, and the producers face a problem in disposing of the spent tea leaves after the extraction. Hence, the utilization of such waste is most desirable. Therefore, the aim of this study was to investigate the potential of spent tea leaves (STL), an abundantly available solid waste, as a non-conventional adsorbent in the removal of a basic dye, methylene blue, from aqueous solutions.

2. Materials and methods

2.1. Adsorbate

The basic dye used in this study was methylene blue (MB) purchased from Sigma–Aldrich (M) Sdn Bhd, Malaysia. The MB was chosen in this study because of its known strong adsorption onto

* Tel.: +604 599 6422; fax: +604 594 1013.
E-mail address: chbassim@eng.usm.my.

0304-3894/$ – see front matter © 2008 Elsevier B.V. All rights reserved.
doi:10.1016/j.jhazmat.2008.04.019

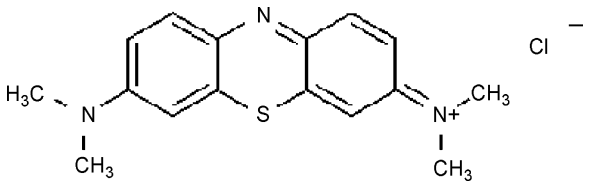

Scheme 1. Chemical structure of methylene blue.

solids. The maximum wavelength of this dye is 668 nm. The structure of MB is shown in Scheme 1.

2.2. Preparation of adsorbent

Spent tea bags were collected from a tea making shop located in the cafeteria of the Engineering Campus, Nibong Tebal, Penang. The spent tea leaves used in this study were removed from the bags and repeatedly boiled with water until the filtered water was cleared. Then it was oven dried at 60 °C for 48 h. The dried sample was ground and sieved to obtain a particle size range of 0.5–1.0 mm and stored in plastic bottle for further use. No other chemical or physical treatments were used prior to adsorption experiments.

2.3. Effect of adsorbent dose

The effect of STL dose on the amount of MB adsorbed was studied by adding different amounts (0.05, 0.10, 0.20, 0.40, 0.60, 0.80, 1.00 and 1.20 g) of STL into a number of 250 mL stoppered glass Erlenmeyers flasks containing a definite volume (200 mL in each flask) of fixed initial concentration (65 mg/L) of dye solution without changing the solution pH at temperature of 30 °C. The flasks were placed in a thermostatic water-bath shaker and agitation was provided at 130 rpm for 180 min. The dye concentrations were measured at equilibrium.

2.4. Equilibrium studies

Adsorption experiments were carried out by adding a fixed amount of sorbent (0.70 g) into a number of 250 mL stoppered glass Erlenmeyers flasks containing a definite volume (200 mL in each flask) of different initial concentrations (30–390 mg/L) of dye solution without changing the solution pH at temperature of 30 °C. The flasks were placed in a thermostatic water-bath shaker and agitation was provided at 130 rpm for 180 min to ensure equilibrium was reached. At time $t = 0$ and equilibrium, the dye concentrations were measured using a double beam UV–vis spectrophotometer (Shimadzu, Model UV 1601, Japan) at 668 nm wavelength. The amount of adsorption at equilibrium, q_e (mg/g), was calculated by:

$$q_e = \frac{(C_0 - C_e)V}{W} \quad (1)$$

where C_0 and C_e (mg/L) are the liquid-phase concentrations of dye at initial and equilibrium, respectively. V (L) is the volume of the solution and W (g) is the mass of dry sorbent used.

The dye removal percentage can be calculated as follows:

$$\text{Removal percentage} = \frac{C_0 - C_e}{C_0} \times 100 \quad (2)$$

where C_0 and C_e (mg/L) are the liquid-phase concentrations of dye at initial and equilibrium, respectively.

2.5. Effect of solution pH

In this study, 200 mL of dye solution of 65 mg/L initial concentration at different pH values (2.0–11.0) was agitated with 0.70 g of STL in a water-bath shaker at 30 °C. Agitation was made for 130 min at a constant agitation speed of 130 rpm. The dye concentrations were measured by a double beam UV–vis spectrophotometer. The pH was adjusted with 0.1N NaOH and 0.1N HCl solutions and measured using a pH meter (Ecoscan, EUTECH Instruments, Singapore).

2.6. Batch kinetic studies

The procedures of kinetic experiments were basically identical to those of equilibrium tests. The aqueous samples were taken at preset time intervals, and the concentrations of dye were similarly measured. All the kinetic experiments were carried out without pH adjustment. The amount of sorption at time t, q_t (mg/g), was calculated by:

$$q_t = \frac{(C_0 - C_t)V}{W} \quad (3)$$

where C_t (mg/L) is the liquid-phase concentration of dye at any time.

2.7. Analytical methods

The dye concentrations were monitored by measuring absorbance at 668 nm using a double beam UV–vis spectrophotometer (Shimadzu, Model UV 1601, Japan). Prior to the measurement, a calibration curve was obtained by using the standard MB solution with known concentrations.

3. Results and discussion

3.1. Effect of adsorbent dose on dye adsorption

To investigate the effect of adsorbent dose (g) on dye adsorption, the experiments were conducted at initial dye concentration of 65 mg/L. Fig. 1 shows the effect of STL dose on the %removal of MB. It was observed that the %removal increased with increase in adsorbent dose. At equilibrium time, the %removal increased from 43.84% to 95.50% for an increase in STL dose from 0.05 to 0.60 g. The increase in %color removal was due to the increase of the available sorption surface and availability of more adsorption sites. Optimum STL dose was found to be 3.50 g of adsorbent per liter of dye solution. A similar observation was previously reported for removal of malachite green dye from aqueous solution by bagasse fly ash and activated carbon [30].

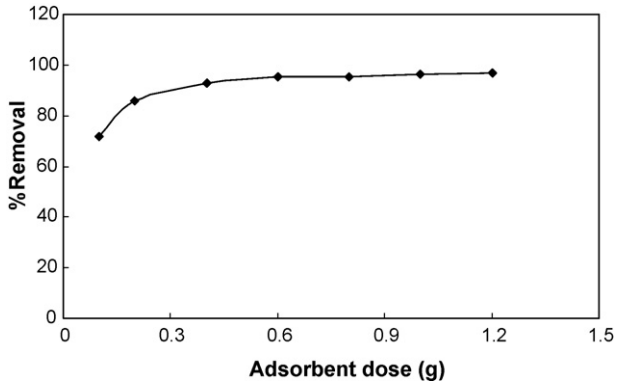

Fig. 1. Effect of adsorbent dosage on the adsorption of MB on STL (temperature = 30 °C, C_0 = 65 mg/L, stirring rate = 130 rpm).

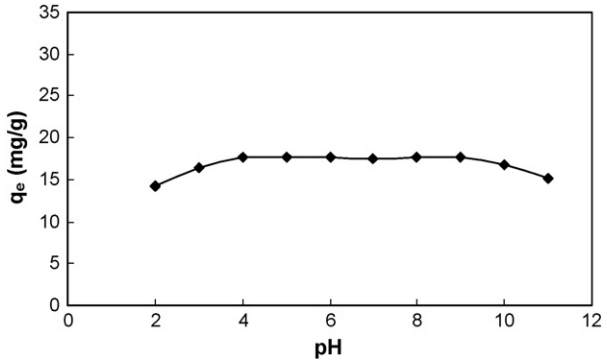

Fig. 2. Effect of solution pH on the adsorption of MB on STL (temperature = 30 °C, C_0 = 65 mg/L, W = 0.70 g/0.20 L solution, stirring rate = 130 rpm).

3.2. Effect of solution pH on dye adsorption

The effect of solution pH on MB adsorption was studied using 0.70 g of STL, 65 mg/L dye initial concentration, pH 2–11 at 30 °C, and the results are shown in Fig. 2. The dye adsorption was slightly changed over the pH value from 2 to 9. The dye adsorption was constant at pH 4–9. The lowest dye adsorption was recorded at pH 2 (15 mg/g). The equilibrium adsorption (q_e) was found to increase with increasing solution pH. The q_e increased from 13 to 85 mg/g for an increase in pH from 2 to 10. Lower adsorption of MB at acidic pH was probably due to the presence of excess H^+ ions competing with the cation groups on the dye for adsorption sites. This, however, did not explain the slight decrease of dye adsorption at higher pH values. There might be another mode of adsorption (ion exchange or chelation for example) [31]. Similar results were reported in the literature [21].

3.3. Effect of contact time and initial concentration on dye adsorption

The effect of initial concentration on the adsorption of MB is shown in Fig. 3. It can be seen that the amount of MB adsorbed per unit mass of adsorbent increased with the increase in initial concentration, although %removal decreased with the increase in initial concentration. The amount of MB adsorbed at equilibrium (q_e) increased from 8.0299 to 102.1376 mg/g as the initial concentration was increased from 30 to 390 mg/L. The initial concentration provides an important driving force to overcome all mass transfer resistances of the MB between the aqueous and solid phases. Hence, a higher initial concentration of dye will enhance the adsorption process. However, the MB %removal decreased from 94.50% to 92.20% as the MB concentration was increased from 30 to 390 mg/L.

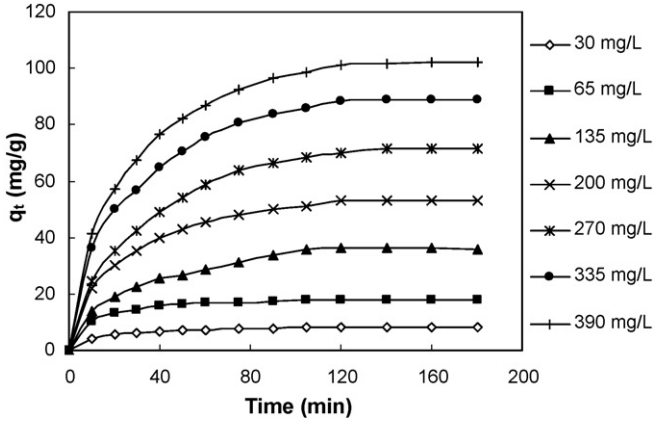

Fig. 3. Effect of contact time and initial concentration on the adsorption of MB on STL (temperature = 30 °C, W = 0.70 g/0.20 L solution, stirring rate = 130 rpm).

Fig. 3 also shows rapid adsorption of MB in the first 30 min for all initial concentrations, and thereafter, the adsorption rate decreases gradually till it reaches equilibrium. The equilibrium conditions were reached within 60–90 min for initial concentrations less than 135 mg/L while 120 min was needed for concentrations from 200 to 390 mg/L. Data on the adsorption kinetics of dyes by various adsorbents have shown a wide range of adsorption rates. For example, the effect of contact time for the adsorption of orange-G and methyl violet dyes by bagasse fly ash was studied for a period of 24 h for initial dye concentrations of 10 mg/L at 30 °C [32]. The authors [32] reported that after 4 h of contact, a steady-state approximation was assumed and a quasi-equilibrium situation was accepted. Doğan et al. [33] reported that equilibrium time of 180 min was enough for the adsorption of methyl violet and methylene blue dyes by sepiolite for initial dye concentration of 1.2×10^{-3} mol/L at 30 °C.

3.4. Isotherm analysis

The equilibrium isotherms in this study were analyzed using the Langmuir, Freundlich and Temkin isotherms. A trial and error procedure was used to determine the three isotherms parameters by minimizing the respective coefficient of determination between experimental data and isotherms using the solver add-in with Microsoft's Excel spreadsheet.

The Langmuir isotherm theory assumes monolayer coverage of adsorbate over a homogenous adsorbent surface [34]. A basic assumption is that sorption takes place at specific homogenous sites within the adsorbent. Once a dye molecule occupies a site, no further adsorption can take place at that site. The Langmuir adsorption isotherm has been successfully used to explain the adsorption of basic dyes from aqueous solutions [7–9].

The Langmuir isotherm is:

$$q_e = \frac{q_m K_a C_e}{1 + K_a C_e} \quad (4)$$

where q_m (mg/g) and K_a (L/mg) are the Langmuir isotherm constants. The equilibrium data were fitted to Langmuir isotherm and the constants together with the R^2 value are listed in Table 1.

The essential characteristics of the Langmuir isotherm can be expressed in terms of a dimensionless constant separation factor R_L that is given by Eq. (5) [35]:

$$R_L = 1/(1 + bC_0) \quad (5)$$

where C_0 is the highest initial concentration of adsorbate (mg/L), and b (L/mg) is Langmuir constant. The value of R_L indicates the shape of the isotherm to be either unfavorable ($R_L > 1$), linear

Table 1
Isotherm constants for MB adsorption on STL at 30 °C

Isotherm	Parameters
Langmuir	
q_m (mg/g)	300.052
K_a (L/mg)	0.0153
R^2	0.9907
Freundlich	
K_F ((mg/g)(L/g)$^{1/n}$	6.4286
n	1.265
R^2	0.9895
Temkin	
A (L/g)	0.5618
B	30.5708
R^2	0.9334

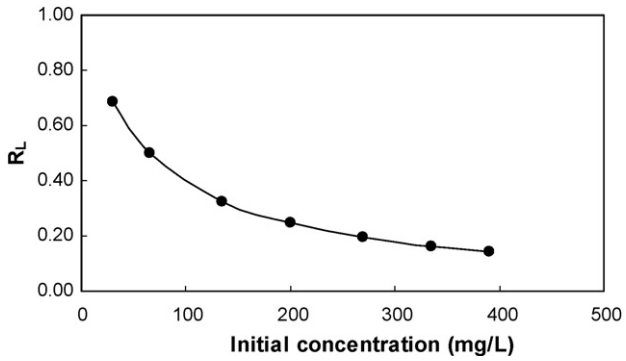

Fig. 4. The separation factor for MB adsorption on STL at 30 °C.

($R_L = 1$), favorable ($0 < R_L < 1$) or irreversible ($R_L = 0$). The R_L values between 0 and 1 indicate favorable adsorption. For adsorption of MB onto STL, R_L values obtained are shown in Fig. 4. The R_L values for the adsorption of MB onto STL are in the range of 0.144–0.685, indicating that the adsorption is a favorable process and that at high initial MB concentrations the adsorption is nearly irreversible.

The Freundlich isotherm [36] is an empirical equation assuming that the adsorption process takes place on heterogeneous surfaces and adsorption capacity is related to the concentration of MB dye at equilibrium:

$$q_e = K_F C_e^{1/n} \tag{6}$$

where K_F (mg/g (L/mg)$^{1/n}$) is roughly an indicator of the adsorption capacity and $1/n$ is the adsorption intensity. The magnitude of the exponent, $1/n$, gives an indication of the favorability of adsorption. Values of $n > 1$ represent favorable adsorption condition [37,38]. The values of K_F, n and the linear regression correlation (R^2) for Freundlich model are given in Table 1.

Temkin and Pyzhev [39] considered the effects of some indirect adsorbate/adsorbate interactions on adsorption isotherms and suggested that because of these interactions the heat of adsorption of all the molecules in the layer would decrease linearly with coverage. The Temkin isotherm has been used in the following form:

$$q_e = \frac{RT}{b} \ln(AC_e) \tag{7}$$

or

$$q_e = B \ln(AC_e) \tag{8}$$

where

$$B = \frac{RT}{b}. \tag{9}$$

The constant B is related to the heat of adsorption. The constants A and B together with the R^2 values are shown in Table 1.

Fig. 5 shows the experimental equilibrium data and the predicted theoretical isotherms for the adsorption of MB onto STL. The calculated isotherm constants by non-linear method are listed in Table 1. It can be seen from Fig. 5 that Langmuir isotherm fits the data better than Freundlich and Temkin isotherms. This is also confirmed by the high value of R^2 in case of Langmuir (0.9907) compared to Freundlich (0.9895) and Temkin (0.9334). This indicates that the adsorption of MB on STL takes place as monolayer adsorption on a surface that is homogenous in adsorption affinity. Table 1 indicates that the computed maximum monolayer adsorption capacity (q_m) of STL for MB was relatively large, which was 300.052 mg/g.

The maximum sorption capacity (q_m) of the STL adsorbent for MB was compared with those reported in literature for different adsorbents/methylene blue adsorption systems as shown in Table 2.

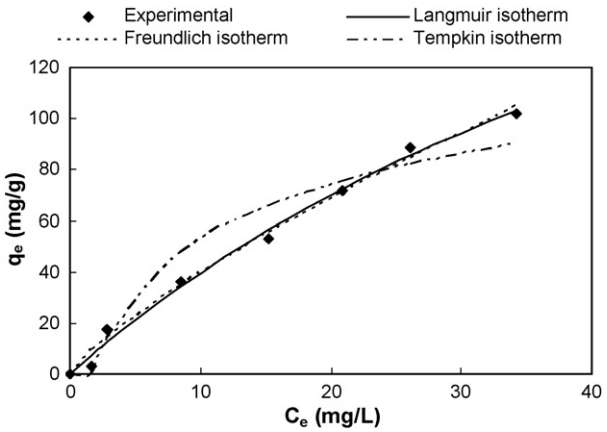

Fig. 5. Isotherm plots for MB adsorption on STL at 30 °C.

The performance of the STL is higher in effectiveness for the removal of MB.

3.5. Adsorption kinetics

The modeling of the kinetics of adsorption of MB on STL was investigated by two common models, namely, the Lagergren pseudo-first-order model and pseudo-second-order model. The pseudo-first-order model was described by Lagergren [46] as:

$$\log(q_e - q_t) = \log q_e - \frac{k_1}{2.303} t \tag{10}$$

where q_e (mg/g) is the amount of MB adsorbed at equilibrium, q_t (mg/g) is the amount of MB adsorbed at time t and k_1 (1/min) is the rate constant of pseudo-first-order adsorption. A linear plot of $\log(q_e - q_t)$ against time allows one to obtain the rate constant (Fig. 6). If the plot was found to be linear with good correlation coefficient, it indicates that Lagergren's equation is appropriate to MB sorption on STL. So, the adsorption process is a pseudo-first-order process [46,47]. The Lagergren's first-order rate constant (k_1) and q_e determined from the model are presented in Table 3, along with the corresponding correlation coefficients. It was observed that the pseudo-first-order model did not fit well. It was found that the calculated q_e values did not agree with the experimental q_e values (Table 3). This suggests that the adsorption of MB did not follow first-order kinetics.

The pseudo-second-order kinetics may be expressed as [48,49]:

$$\frac{t}{q_t} = \frac{1}{k_2 q_e^2} + \frac{1}{q_e} t \tag{11}$$

Table 2
Comparison of monolayer equilibrium capacity for methylene blue onto other different adsorbents

Adsorbent	q_m (mg/g)	Reference
Spent tea leaves	300.052	This work
Coffee husks	90.09	[40]
Luffa cylindrica fibers	47	[41]
Guava (*Psidium guajava*) leaf powder	295.04	[42]
Fallen phoenix tree's leaves	83.8 ± 7.6	[43]
Dehydrated wheat bran carbon	185.2	[44]
Activated *Rosa canina* seeds (500 °C)	47.2	[45]
Rattan-based activated carbon	294.12	[9]
Oil palm fibre activated carbon	277.78	[8]

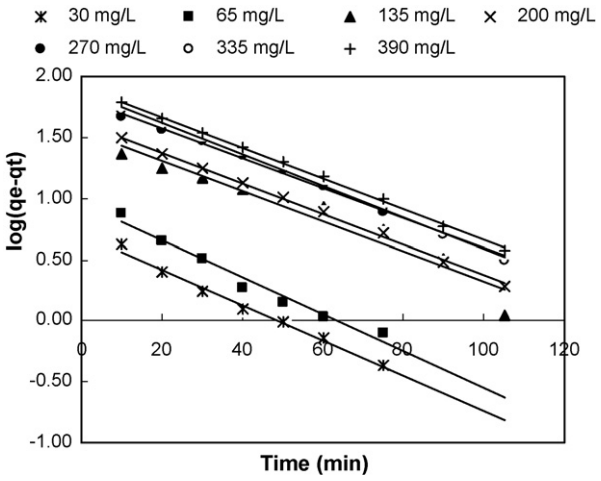

Fig. 6. The fitting of pseudo-first-order model for MB on STL for different initial concentrations at 30 °C.

where the equilibrium adsorption capacity (q_e) and the second-order constant k_2 (g/mg min) can be determined experimentally from the slope and intercept of plot t/q_t versus t (Fig. 7). The k_2 and q_e determined from the model are presented in Table 3 along with the corresponding correlation coefficients. The values of the calculated and experimental q_e are presented in Table 3. It can be seen from Table 3 that the pseudo-second-order model better represented the adsorption kinetics, suggesting that the adsorption process was controlled by chemisorption. A similar result was reported for the adsorption of methylene blue from aqueous solution onto acid-activated andesite [50].

The initial adsorption rates h (mg/g min) can be calculated from the pseudo-second-order model by the following equation:

$$h_{0,2} = k_2 q_e^2 \quad (12)$$

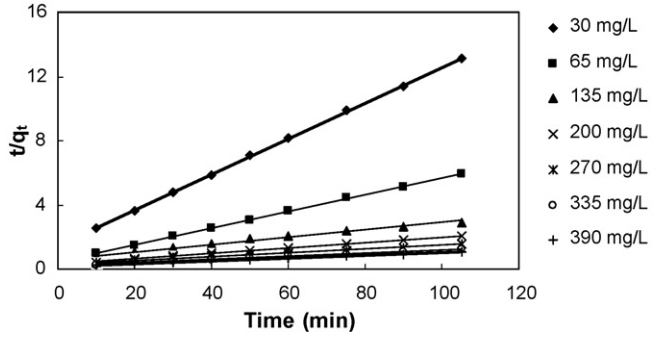

Fig. 7. The fitting of pseudo-second-order model for MB on STL for different initial concentrations at 30 °C.

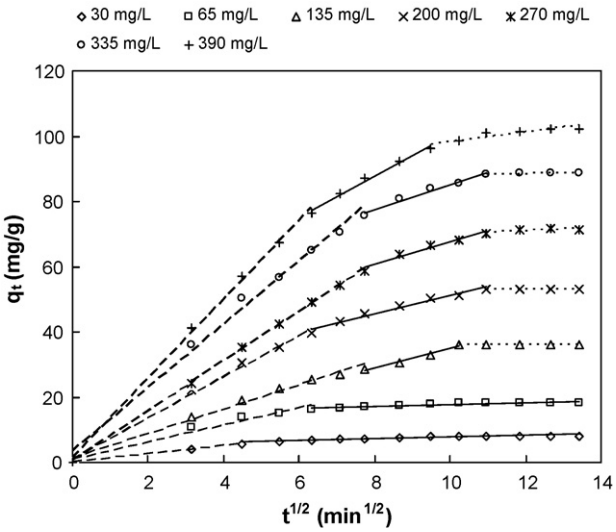

Fig. 8. Intraparticle diffusion plot for MB adsorption on STL for different initial concentrations at 30 °C.

and the results are listed in Table 3. It was found that the initial rate of adsorption increases with increasing initial MB concentration, which would be expected due to the increase in driving force at higher concentration.

3.6. Intraparticle diffusion

As the above kinetic models were not able to identify the diffusion mechanism, thus intraparticle diffusion model based on the theory proposed by Weber and Morris [51] was tested. It is an empirically found functional relationship, common to the most adsorption processes, where uptake varies almost proportionally with $t^{1/2}$ rather than with the contact time t. According to this theory:

$$q_t = k_{pi} t^{1/2} + C_i \quad (13)$$

where k_{pi} (mg/g min$^{1/2}$), the rate parameter of stage i, is obtained from the slope of the straight line of q_t versus $t^{1/2}$ (Fig. 8). The values of k_{pi}, C_i and correlation coefficient, R^2 obtained for the plots are given in Table 4. C_i, the intercept of stage i, gives an idea about the thickness of boundary layer, i.e., the larger the intercept, the greater the boundary layer effect. If intraparticle diffusion occurs, then q_t versus $t^{1/2}$ will be linear and if the plot passes through the origin, then the rate limiting process is only due to the intraparticle diffusion. Otherwise, some other mechanism along with intraparticle diffusion is also involved [52]. For intraparticle diffusion plots, the first, sharper region is the instantaneous adsorption or external surface adsorption. The second region is the gradual adsorption stage where intraparticle diffusion is the rate limiting. In some cases,

Table 3
Comparison of the pseudo-first-order, pseudo-second-order adsorption rate constants and calculated and experimental q_e values obtained at different initial MB concentrations

Initial concentration (mg/L)	$q_{e,exp}$ (mg/g)	Pseudo-first-order kinetic model			Pseudo-second-order kinetic model			
		k_1 (1/min)	$q_{e,cal}$ (mg/g)	R^2	k_2 (g/mg min) 10^4	$q_{e,cal}$ (mg/g)	R^2	h_0
30	8.029	0.0322	5.146	0.9904	84.50	8.993	0.9998	0.6833
65	17.778	0.0335	9.185	0.9715	57.20	19.268	0.9997	2.123
135	35.999	0.0273	36.392	0.9331	8.54	43.478	0.9875	1.614
200	53.157	0.0278	42.423	0.9979	8.18	60.976	0.9985	3.041
270	71.436	0.0273	66.973	0.9974	3.84	87.719	0.9967	2.955
335	88.740	0.0284	75.527	0.9965	4.45	103.093	0.9969	4.729
390	102.140	0.0278	83.291	0.9986	4.06	117.647	0.9987	5.619

Table 4
Intraparticle diffusion model constants and correlation coefficients for adsorption of MB on STL at 30 °C

Initial concentration (mg/L)	k_{p1} (mg/g min$^{1/2}$)	C_1	$(R_1)^2$	k_{p2} (mg/g min$^{1/2}$)	C_2	$(R_2)^2$	k_{p3} (mg/g min$^{1/2}$)	C_3	$(R_3)^2$
30	1.229	−0.006	1.000	0.259	5.042	0.823	–	–	–
65	2.611	0.9563	0.968	0.265	15.033	0.822	–	–	–
135	3.337	2.623	0.981	2.908	47.395	0.977	0.022	5.6804	0.126
200	6.336	0.900	0.995	2.776	85.908	0.978	0.014	23.294	0.669
270	7.637	0.289	0.999	3.460	32.857	0.968	0.476	65.318	0.625
335	9.704	3.101	0.991	3.833	46.688	0.979	0.202	86.172	0.59
390	12.131	1.268	0.997	6.2864	37.445	0.990	1.465	83.522	0.833

the third region exists, which is the final equilibrium stage where intraparticle diffusion starts to slow down due to the extremely low adsorbate concentrations left in the solutions [52]. Referring to Fig. 8, for all initial concentrations, the first stage was completed within the first 40 min and the second stage of intraparticle diffusion control was then attained. The third stage only occurred for higher MB initial concentration of 135, 200, 270, 335 and 390 mg/L. The different stages of rates of adsorption observed indicated that the adsorption rate was initially faster and then slowed down when the time increased. As seen from Fig. 8, the plots were not linear over the whole time range, implying that more than one process affected the adsorption.

3.7. SEM of adsorbent

Fig. 9 shows the SEM micrographs of STL samples before and after dye adsorption. Fig. 9a shows that the STL possesses a rough surface morphology with pores of different sizes. These pores are useful for dye adsorption. The surface of dye-loaded adsorbent (Fig. 9b), however, shows that the surface of STL is covered with dye molecules.

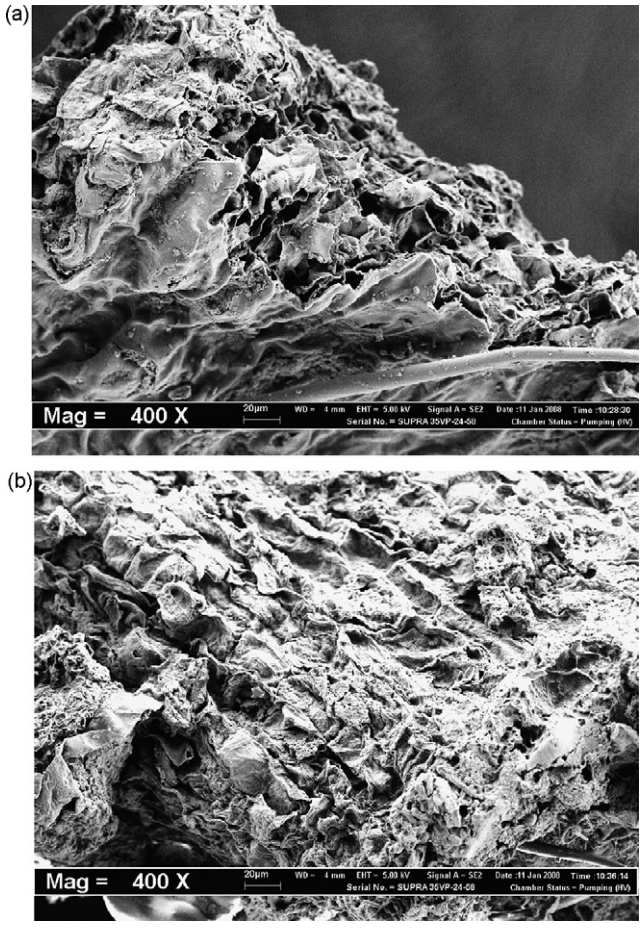

Fig. 9. SEM micrograph of STL particle (magnification: 400×): (a) before dye sorption and (b) with dye adsorbed.

4. Conclusions

The results obtained show that the spent tea leaves, an abundantly available waste, can be used for the removal of MB from aqueous solution. The equilibrium data were fitted to non-linear models of Langmuir, Freundlich and Temkin, and the equilibrium data were best described by the Langmuir isotherm model, with maximum monolayer adsorption capacity of 300.052 mg/g of STL at 30 °C. Kinetic data were tested using the pseudo-first-order and pseudo-second-order kinetic models. The kinetics of the adsorption process was found to follow the pseudo-second-order kinetic model, suggesting that the adsorption process was controlled by chemisorption. The plots of intraparticle diffusion model were not linear over the whole time range, implying that more than one process affected the adsorption. The spent tea leaves used in this work are freely and abundantly available, do not require an additional pretreatment step such as activation before applications and possess high adsorption capacity for MB. Therefore, the adsorbent is expected to be economically feasible for removal of MB dye from aqueous solutions.

Acknowledgement

The author acknowledges the research grant provided by the Universiti Sains Malaysia under the Research University (RU) Scheme (Project no: 1001/PJKIMIA/814005).

References

[1] A. Durán, J.M. Monteagudo, E. Amores, Solar photo-Fenton degradation of Reactive Blue 4 in a CPC reactor, Appl. Catal. B: Environ. 80 (2008) 42–50.
[2] J. Sun, L. Qiao, S. Sun, G. Wang, Photocatalytic degradation of Orange G on nitrogen-doped TiO_2 catalysts under visible light and sunlight irradiation, J. Hazard. Mater. 155 (2008) 312–319.
[3] J. García-Montaño, N. Ruiz, I. Muñoz, X. Domènech, J.A. García-Hortal, F. Torrades, J. Peral, Environmental assessment of different photo-Fenton approaches for commercial reactive dye removal, J. Hazard. Mater. 138 (2006) 218–225.
[4] W. Azmi, R.K. Sani, U.C. Banerjee, Biodegradation of triphenylmethane dyes, Enzyme Microb. Technol. 22 (1998) 185–191.
[5] G. Sudarjanto, B. Keller-Lehmann, J. Keller, Optimization of integrated chemical–biological degradation of a reactive azo dye using response surface methodology, J. Hazard. Mater. 138 (2006) 160–168.
[6] L. Fan, Y. Zhou, W. Yang, G. Chen, F. Yang, Electrochemical degradation of aqueous solution of Amaranth azo dye on ACF under potentiostatic model, Dyes Pigments 76 (2008) 440–446.
[7] B.H. Hameed, A.T.M. Din, A.L. Ahmad, Adsorption of methylene blue onto bamboo-based activated carbon: kinetics and equilibrium studies, J. Hazard. Mater. 141 (2007) 819–825.
[8] I.A.W. Tan, B.H. Hameed, A.L. Ahmad, Equilibrium and kinetic studies on basic dye adsorption by oil palm fibre activated carbon, Chem. Eng. J. 127 (2007) 111–119.
[9] B.H. Hameed, A.L. Ahmad, K.N.A. Latiff, Adsorption of basic dye (methylene blue) onto activated carbon prepared from rattan sawdust, Dyes Pigments 75 (2007) 143–149.

[10] A. Kumar, S. Kumar, S. Kumar, D.V. Gupta, Adsorption of phenol and 4-nitrophenol on granular activated carbon in basal salt medium: equilibrium and kinetics, J. Hazard. Mater. 147 (2007) 155–166.
[11] O. Hamdaoui, E. Naffrechoux, Modeling of adsorption isotherms of phenol and chlorophenols onto granular activated carbon. Part II. Models with more than two parameters, J. Hazard. Mater. 147 (2007) 401–411.
[12] N. Daneshvar, S. Aber, A. Khani, A.R. Khataee, Study of imidaclopride removal from aqueous solution by adsorption onto granular activated carbon using an on-line spectrophotometric analysis system, J. Hazard. Mater. 144 (2007) 47–51.
[13] C.P. Dwivedi, J.N. Sahu, C.R. Mohanty, B. Raj Mohan, B.C. Meikap, Column performance of granular activated carbon packed bed for Pb(II) removal, J. Hazard. Mater. 156 (2008) 596–603.
[14] J.H. Tsai, H.M. Chiang, G.Y. Huang, H.L. Chiang, Adsorption characteristics of acetone, chloroform and acetonitrile on sludge-derived adsorbent, commercial granular activated carbon and activated carbon fibers, J. Hazard. Mater. 154 (2008) 1183–1191.
[15] A.A. Ahmad, B.H. Hameed, N. Aziz, Adsorption of direct dye on palm ash: kinetic and equilibrium modeling, J. Hazard. Mater. 141 (2007) 70–76.
[16] B.H. Hameed, A.A. Ahmad, N. Aziz, Isotherms, kinetics and thermodynamics of acid dye adsorption on activated palm ash, Chem. Eng. J. 133 (2007) 195–203.
[17] M. Hasan, B.H. Hameed, A.L. Ahmad, Adsorption of reactive dye onto cross-linked chitosan/oil palm ash composite beads, Chem. Eng. J. 136 (2008) 164–172.
[18] B.H. Hameed, D.K. Mahmoud, A.L. Ahmad, Sorption of basic dye from aqueous solution by Pomelo (*Citrus grandis*) peel in a batch system, Colloids Surf. A: Physicochem. Eng. Aspects 316 (2008) 78–84.
[19] B.H. Hameed, M.I. El-Khaiary, Removal of basic dye from aqueous medium using a novel agricultural waste material: pumpkin seed hull, J. Hazard. Mater. 155 (2008) 601–609.
[20] B.H. Hameed, M.I. El-Khaiary, Sorption kinetics and isotherm studies of a cationic dye using agricultural waste: broad bean peels, J. Hazard. Mater. 154 (2008) 639–648.
[21] B.H. Hameed, M.I. El-Khaiary, Batch removal of malachite green from aqueous solutions by adsorption on oil palm trunk fibre: equilibrium isotherms and kinetic studies, J. Hazard. Mater. 154 (2008) 237–244.
[22] B.H. Hameed, H. Hakimi, Utilization of durian (*Durio zibethinus* Murray) peel as low cost sorbent for the removal of acid dye from aqueous solutions, Biochem. Eng. J. 39 (2008) 338–343.
[23] P.P. Selvam, S. Preethi, P. Basakaralingam, N. Thinakaran, A. Sivasamy, S. Sivanesan, Removal of rhodamine B from aqueous solution by adsorption onto sodium Montmorillonite, J. Hazard. Mater. 155 (2008) 39–44.
[24] F.A. Batzias, D.K. Sidiras, Simulation of methylene blue adsorption by salts-treated beech sawdust in batch and fixed-bed systems, J. Hazard. Mater. 149 (2007) 8–17.
[25] Z. Bekçi, C. Özveri, Y. Seki, K. Yurdakoç, Sorption of malachite green on chitosan bead, J. Hazard. Mater. 154 (2008) 254–261.
[26] P. Pengthamkeerati, T. Satapanajaru, O. Singchan, Sorption of reactive dye from aqueous solution on biomass fly ash, J. Hazard. Mater. 153 (2008) 1149–1156.
[27] S.K. Alpat, Ö. Özbayrak, Ş. Alpat, H. Akçay, The adsorption kinetics and removal of cationic dye, Toluidine Blue O, from aqueous solution with Turkish zeolite, J. Hazard. Mater. 151 (2008) 213–220.
[28] F. Doulati Ardejani, Kh. Badii, N. Yousefi Limaee, S.Z. Shafaei, A.R. Mirhabibi, Adsorption of Direct Red 80 dye from aqueous solution onto almond shells: effect of pH, initial concentration and shell type, J. Hazard. Mater. 151 (2008) 730–737.
[29] N.S. Mokgalaka, R.I. McCrindle, B.M. Botha, Multielement analysis of tea leaves by inductively coupled plasma optical emission spectro metry using slurry nebulization, J. Anal. Atomic Spectrom. 19 (2004) 1375–1378.
[30] I.D. Mall, V.C. Srivastava, N.K. Agarwal, I.M. Mishra, Adsorptive removal of malachite green dye from aqueous solution by bagasse fly ash and activated carbon-kinetic study and equilibrium isotherm analyses, Colloids Surf. A: Physicochem. Eng. Aspects 264 (2005) 17–28.
[31] O. Hamdaoui, Batch study of liquid-phase adsorption of methylene blue using cedar sawdust and crushed brick, J. Hazard. Mater. B135 (2006) 264–273.
[32] I.D. Mall, V.C. Srivastava, N.K. Agarwal, Removal of Orange-G and Methyl Violet dyes by adsorption onto bagasse fly ash-kinetic study and equilibrium isotherm analyses, Dyes Pigments 69 (2006) 210–223.
[33] M. Doğan, Y. Özdemir, M. Alkan, Adsorption kinetics and mechanism of cationic methyl violet and methylene blue dyes onto sepiolite, Dyes Pigments 75 (2007) 701–713.
[34] I. Langmuir, The adsorption of gases on plane surfaces of glass, mica and platinum, J. Am. Chem. Soc. 40 (1918) 1361–1403.
[35] K.R. Hall, L.C. Eagleton, A. Acrivos, T. Vermeulen, Pore-and solid-diffusion kinetics in fixed-bed adsorption under constant-pattern conditions, I&EC Fundam. 5 (1966) 212–223.
[36] H. Freundlich, Über die adsorption in lösungen (Adsorption in solution), Z. Phys. Chem. 57 (1906) 384–470.
[37] R.E. Treybal, Mass Transfer Operations, second ed., McGraw Hill, New York, 1968.
[38] Y.S. Ho, G. McKay, Sorption of dye from aqueous solution by peat, Chem. Eng. J. 70 (1978) 115–124.
[39] M.J. Temkin, V. Pyzhev, Recent modifications to Langmuir Isotherms, Acta Physiochim. USSR 12 (1940) 217–222.
[40] L.S. Oliveira, A.S. Franca, T.M. Alves, S.D.F. Rocha, Evaluation of untreated coffee husks as potential biosorbents for treatment of dye contaminated waters, J. Hazard. Mater. 155 (2008) 507–512.
[41] H. Demir, A. Top, D. Balköse, S. Ülkü, Dye adsorption behavior of *Luffa cylindrica* fibers, J. Hazard. Mater. 153 (2008) 389–394.
[42] V. Ponnusami, S. Vikram, S.N. Srivastava, Guava (*Psidium guajava*) leaf powder: novel adsorbent for removal of methylene blue from aqueous solutions, J. Hazard. Mater. 152 (2008) 276–286.
[43] R. Han, W. Zou, W. Yu, S. Cheng, Y. Wang, J. Shi, Biosorption of methylene blue from aqueous solution by fallen phoenix tree's leaves, J. Hazard. Mater. 141 (2007) 156–162.
[44] A. Özer, G. Dursun, Removal of methylene blue from aqueous solution by dehydrated wheat bran carbon, J. Hazard. Mater. 146 (2007) 262–269.
[45] A. Gürses, Ç. Doğar, S. Karaca, M. Açikyildiz, R. Bayrak, Production of granular activated carbon from waste *Rosa canina* sp. seeds and its adsorption characteristics for dye, J. Hazard. Mater. B131 (2006) 254–259.
[46] S. Lagergren, About the theory of so-called adsorption of soluble substances, K. Sven. Vetenskapsakad. Handl. 24 (4) (1898) 1–39.
[47] Y.S. Ho, G. McKay, The sorption of lead (II) ions on peat, Water Res. 33 (1999) 578–584.
[48] Y.S. Ho, G. McKay, Sorption of dye from aqueous solution by peat, Chem. Eng. J. 70 (1998) 115–124.
[49] Y.S. Ho, G. McKay, The kinetics of sorption of divalent metal ions onto sphagnum moss peat, Water Res. 34 (2000) 735–742.
[50] W.T. Tsai, H.C. Hsu, T.Y. Su, K.Y. Lin, C.M. Lin, T.H. Dai, The adsorption of cationic dye from aqueous solution onto acid-activated andesite, J. Hazard. Mater. 147 (2007) 1056–1062.
[51] W.J. Weber, J.C. Morris, Kinetics of adsorption on carbon from solution, J. Sanitary Eng. Division, Am. Soc. Chem. Eng. 89 (1963) 31–59.
[52] W.H. Cheung, Y.S. Szeto, G. McKay, Intraparticle diffusion processes during acid dye adsorption onto chitosan, Bioresour. Technol. 98 (2007) 2897–2904.